Journal of the Ceramic Society of Japan **115** [5] 310–314 (2007)

Visible-Light-Induced Hydrophilic Conversion of an S-Doped TiO_2 Thin Film and Its Photocatalytic Activity for Decomposition of Acetaldehyde in Gas Phase

Kazumoto NISHIJIMA, Hitoshi NAITOH, Toshiki TSUBOTA and Teruhisa OHNO

Department of Applied Chemistry, Faculty of Engineering, Kyushu Institute of Technology,
1-1, Sensui-cho, Tobata-ku, Kitakyushu-shi 804-8550

S-doped titanium dioxide thin films were found to undergo hydrophilic conversion under visible light irradiation. The water contact angle for the S-doped TiO_2 thin film reached to 15° under visible light irradiation. The photocatalyzed decomposition of acetaldehyde (ALD) in gas phase on TiO_2 thin films was investigated in a batch-type photocatalytic reactor. The photocatalytic activities of TiO_2 thin films for decomposition of ALD were investigated by analyzing amount of ALD consumed and CO_2 generated under visible light irradiation at wavelengths longer than 420 nm.

[Received November 11, 2006; Accepted March 22, 2007]

Key-words : *Photoinduced hydrophilicity, Photocatalysts, Titanium dioxide, S-doped titanium dioxide, Visible light, Degradation of acetaldehyde*

1. Introduction

TiO_2 coating materials has attracted much attention as a high active photocatalyst in recent years because of its potential for degradation of pollutant.[1)] TiO_2 thin films reveals a photoinduced highly hydrophilic conversion on its surface.[2),3)] In addition, irradiation with UV light causes conventional photocatalytic oxidation reactions on the film surface.[4)-9)] These reactions result in useful properties such as self-cleaning, antifogging, and antibacterial functions.[10)]

The surface properties of TiO_2 show superhydrophilicity under ultraviolet (UV) light irradiation[2),3),11)-14)] with a water contact angle reaching 0°. This phenomenon has previously been applied to various products, including self-cleaning tiles and anti-fogging mirrors.[15)] However, these applications are limited to outdoor use because the photoinduced superhydrophilic conversion and photocatalytic degradation of odors requires UV light irradiation of approximately the same intensity as that of natural sunlight.

Application of TiO_2 photocatalysis is a promising techniques for decomposing organic contaminations at low concentrations in the air.[1),16),17)] There have been few studies on degradation and decomposition of organic compounds on a TiO_2 thin film under visible light. Therefore, the photocatalytic decomposition of gas phase acetaldehyde (ALD, used as a model substance) on a TiO_2 thin film was investigated with the aim of determining the dependence of incident light wavelength.

N-doped TiO_2 powders and thin films have been reported to show photocatalytic activity and photoinduced hydrophilic properties under visible (VIS) light irradiation.[18)-20)] Sakatani et al. reported photocatalytic decomposition of acetaldehyde on doped TiO_2 photocatalyst powder under VIS light irradiation, which is presumed to be N-doped TiO_2.[18)] Asahi et al. reported results of theoretical calculation of the band structure of nitrogen-substituted TiO_2 and its VIS light-induced photocatalysis when using powders and thin films.[19)] However, Asahi et al. only evaluated the photoinduced hydrophilic property of an N-doped TiO_2 thin film under interior lighting. Irie et al. reported that the surfaces of N-substituted TiO_2 films with various degrees of nitrogen substitution became hydrophilic under VIS light irradiation.[20)]

It has recently been revealed that S-doped TiO_2 powder photocatalysts show the activity for oxidation of organic compounds under visible light irradiation.[21)-24)] However, photoinduced hydrophilicity and photocatalytic activity of S-doped TiO_2 thin films have not been reported. We confirmed that the surface of an S-doped TiO_2 films underwent hydrophilic conversion under VIS light irradiation and that an S-doped TiO_2 thin film has photocatalytic activity for degradation of acetaldehyde to evolve CO_2 under photoirradiation at a wavelength longer than 350 nm.

2. Experimental

2.1 Materials and instruments

Titanium dioxide (TiO_2) powder (ST-01) having an anatase phase was obtained from Ishihara Sangyo. The relative surface area of ST-01 was 310.5 m^2/g. A dispersing reagent (POIZ 532A) was obtained from Kao Chemical Corporation. Acetaldehyde (ALD) was purchased from Wako Pure Chemical Ltd. S-doped TiO_2 powders as starting materials were synthesized by previously reported methods.[21)-24)]

The crystal structures of TiO_2 powders were determined from X-ray diffraction (XRD) patterns measured by using an X-ray diffractometer (Philips, X'Pert-MRD) with a Cu target $K\alpha$-ray ($\lambda = 0.154$ nm). The relative surface areas of the powders were determined by N_2 adsorption/desorption isotherm analysis (BET method). The measurements were performed using a Micromeritics FlowSorb II 2300. The absorption and diffuse reflection spectra were measured using a Shimadzu UV-2500PC spectrophotometer. X-ray photoelectron spectra (XPS) of the TiO_2 powders were measured using a JEOL JPS90SX photoelectron spectrometer with an Al $K\alpha$ source (1486.6 eV). The shift of binding energy due to relative surface charging was corrected using the C 1s level at 285 eV as an internal standard. The XPS peaks were assumed to have Gaussian line shapes and were resolved into components by a non-linear least-squares procedure after proper subtraction of the baseline. The surface roughness factors of the TiO_2 thin films were determined by an atomic force microscope (AFM, Digital Instruments NanoScope III).

2.2 Preparation of TiO_2 coating solution

TiO_2 powder sample (1.5 g) such as S-doped TiO_2 or pure TiO_2 was mixed with 0.15 g of dispersing reagent (POIZ) and 15 g of water. The mixture was put into a zirconia pot (45 cm^3 in inner volume) with zirconia beads (15 g) of 0.6 mm in diameter. A high-energy planetary mill (Pulverisette-7, Fritsch, Germany) operated at a rotation speed of 700 rpm rotation speed for 10 h was used for grinding the mixture at room temperature. A highly dispersed solution was obtained after this treatment.

2.3 Preparation of TiO_2 thin films

TiO_2 thin films with thicknesses of 200 to 400 nm were prepared on one side of silica-coated soda lime glass (5.0 cm × 7.5 cm) by a spin-coating process (Nanotech, SC308) using a freshly prepared coating solution as described above. The spin rate was controlled to produce a 100-nm-thick film for each spin-coating process. Prior to deposition, the substrates were ultrasonically cleaned with ethanol for 3 min, rinsed with distilled water, and dried with air spray. The coating procedures were repeated two to five times. After each procedure, the coated sample was dried at 60°C for 40 min. Finally, the sample was irradiated by black light for 2 h to remove the dispersing reagent (POIZ). The XPS spectra of TiO_2 thin film prepared with or without using POIZ were observed in order to confirm the removal of POIZ after black light irradiation. C/Ti values for the thin film without using POIZ and the thin film with using POIZ were 0.85 and 0.86, respectively. These results suggested that POIZ was perfectly removed after black light irradiation. Surface morphologies and crystal structures of S-doped TiO_2 thin films were observed by scanning electron microscopy (SEM), atomic force microscopy (AFM) and X-ray diffractometer (XRD).

2.4 Evaluation of hydrophilicity on S-doped TiO_2 thin film under photoirradiation

The photoinduced hydrophilicity was evaluated by analysis of the change in water contact angles under photoirradiation at various wavelengths. Several water droplets of 1.5 μL in volume were spread on the samples and water contact angles were measured at 3 points of the thin film surface. The thin film was photoirradiated using a 500 W Xe lamp (USHIO Co. Ltd., OPTICAL MODULEX SX-UI500XQ) that emits both UV light and visible light over a wide wavelength range. To limit the irradiation wavelength, the light beam was passed through a UV-35, L-42, Y-44, Y-50 or Y-54 filter (Kenko Co.) to cut off wavelengths shorter than 350, 420, 440, 500 or 540 nm, respectively. Fine stainless meshes were used as neutral density filters to adjust the irradiation intensity. Prior to light irradiation, all of the S-doped TiO_2 thin films showed water contact angles of around 30°, which were taken as the initial water contact angles. Hydrophobicity of the surface of TiO_2 thin film was recovered by heat-treatment under aerated condition for 4 h.

2.5 Photocatalytic decomposition of ALD on S-doped TiO_2 thin films under photoirradiation

Photocatalytic decomposition of ALD was carried out in a 125-ml tedler bag. A TiO_2-coated glass substrate of 2.5 cm × 2.5 cm in size, obtained by cutting the original 5.0 cm × 7.5 cm substrate, was utilized as the photocatalyst and placed in the tedler bag.

The procedure used for photocatalytic decomposition of ALD is as follows. First, 500 ppm of gas-phase ALD-containing synthetic air was prepared by injecting an appropriate amount of ALD liquid into a tedlar bag containing 125 ml of synthetic air at room temperature. The tedler bag was kept at room temperature until the ALD liquid had completely evaporated. An S-doped TiO_2-coated soda lime glass (2.5 cm × 2.5 cm) was placed in a new tedler bag. The air in the tedler bag was completely removed by using vacuum pump. ALD-containing synthetic air (500 ppm, 125 ml) was introduced into the tedler bag in which the S-doped TiO_2-coated soda lime grass had been placed. The tedler bag was photoirradiated using a 500 W Xe lamp (USHIO Co. Ltd., OPTICAL MODULEX SX-UI500XQ) that emits both UV and visible light over a wide wavelength range. To limit the irradiation wavelength, the light beam was passed through a UV-35 or L-42 filter (Kenko Co.) to cut off wavelengths shorter than 350 or 420 nm, respectively. Fine stainless meshes were used as neutral density filters to adjust the irradiation intensity. The amount of acetaldehyde decomposed by photocatalytic reactions was determined using a gas chromatograph (SHIMADZU GC-8A, FID detector) equipped with a PEG-20M 20% Celite 545 60/80 packed glass column using C-R8A CHROMATOPAC for data processing. In addition, the amount of CO_2 evolved by photocatalytic reactions was determined using a gas chromatograph (SHIMADZU GC-9A, FID detector) instrumented with a TCP 20% Uniport R 60/80 packed column and an MT-221 METHANIZER and using Smart Chrom (KYA Technologies Co.) data processing.

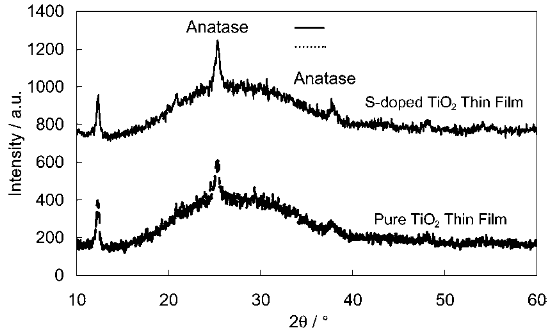

Fig. 1. XRD peaks of S-doped TiO_2 and pure TiO_2 thin films.

3. Results and discussion

3.1 Physical properties of S-doped TiO_2 thin film

X-ray diffraction patterns (XRD) of the obtained S-doped TiO_2 thin films were assigned to mainly anatase structure as shown in **Fig. 1**. These results suggested that the crystal structure of S-doped TiO_2 powders that were originally anatase phase is stable even after high-energy planetary mill treatment.

Figure 2 shows the optical spectrum of S-doped TiO_2 and pure-anatase TiO_2 (ST-01) powder used for preparing thin films.[21)-24)] Noticeable shifts of the absorbance to the visible-light region were observed for the S-doped TiO_2 powder.

Figures 3 and **4** show surface morphologies observed by scanning electron microscopy (SEM) and atomic force microscopy (AFM), respectively. All AFM images of the samples were obtained in a tapping mode at a driving frequency of about 300 kHz and a scan rate of 1.0 Hz. Grain sizes and surface roughness factors (R_a) of S-doped TiO_2 were identical, 20–30 nm and 11.2 nm ($\sigma = 0.799$ nm), respectively. The pure TiO_2 thin film had grain sizes of 10–20 nm and Ra of 16.2 nm ($\sigma = 1.498$ nm).

Densities of thin films calculated from weight, areas and thickness of pure TiO_2 and S-doped TiO_2 thin films were 2.8 g/cm^3 and 3.6 g/cm^3, respectively (Density of TiO_2 having anatase phase is 3.9 g/cm^3).

In order to identify the oxidation states of S atoms and determine the atom% of S atoms incorporated into the bulk of S-doped TiO_2, S 1s Ti 1s, and O 1s core levels were measured by X-ray photoemission spectroscopy (XPS). A peak at 168 eV assigned to S^{4+} was observed. In addition, this peak remained after Ar etching for 20 min. These results suggested that S^{4+} atoms were incorporated into the bulk of TiO_2. From the results of XPS spectra, the amount of S atoms in S-doped

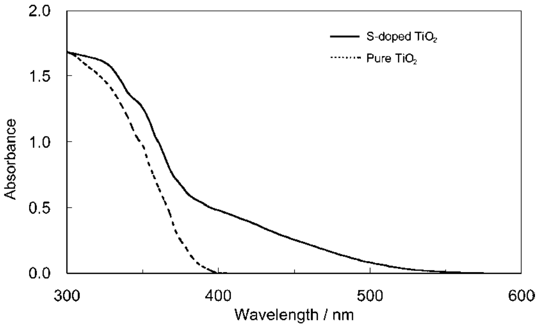

Fig. 2. Diffuse reflectance spectra of S-doped TiO_2 and pure TiO_2. Both TiO_2 photocatalysts have an anatase phase.

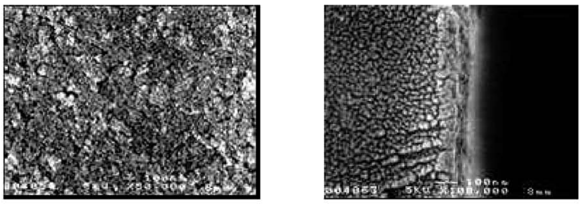

(a) 1 time coat (Surface) (b) 1 time coat (Cross Section)

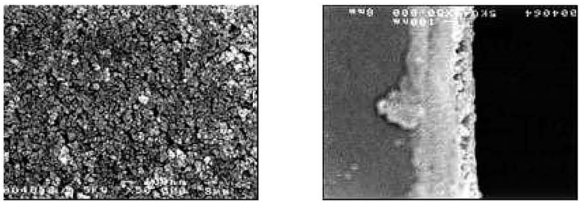

(c) 3 times coat (Surface) (d) 3 times coat (Cross Section)

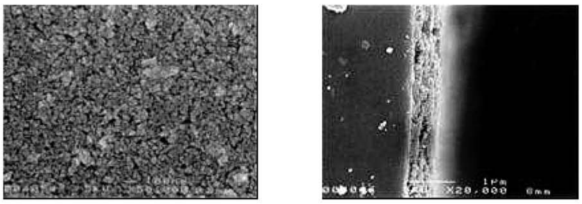

(e) 5 times coat (Surface) (f) 5 times coat (Cross Section)

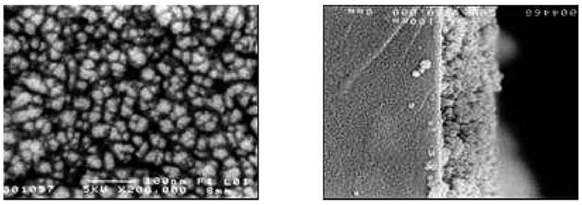

(g) Pure TiO_2 (Surface) (h) Pure TiO_2 (Cross Section)

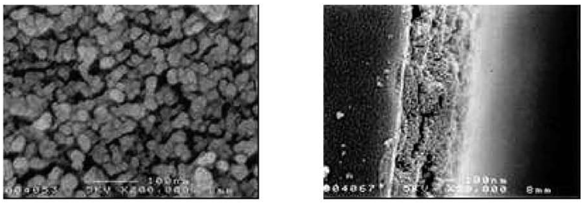

(i) S-doped TiO_2 (Surface) (j) S-doped TiO_2 (Cross Section)

Fig. 3. SEM images of S-doped TiO_2 and pure TiO_2 thin films. (a)-(f) Relationship between coating times and thickness of thin films (surface morphologies and cross sections of thin films). (g) Pure TiO_2 thin film (surface), (h) pure TiO_2 (cross section), (i) S-doped TiO_2 (surface), (j) S-doped TiO_2 (cross section).

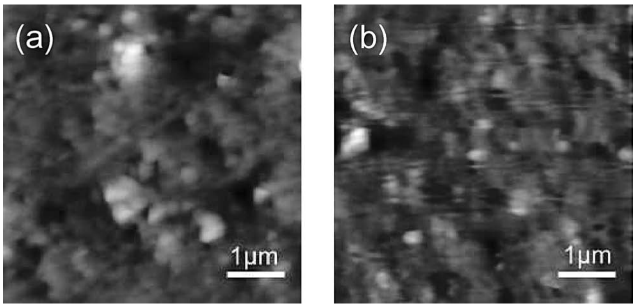

Fig. 4. AFM images of S-doped TiO_2 and pure TiO_2 thin films. (a) S-doped TiO_2 thin film, (b) pure TiO_2 thin film.

TiO_2 was determined to 1.0 atom%.

3.2 Photoinduced hydrophilicity of S-doped TiO_2 thin film

Changes in water contact angles on S-doped TiO_2 and pure TiO_2 thin films were observed under photoirradiation at wavelengths longer than 350 nm as shown in **Fig. 5**. Incident light intensities under photoirradiation at wavelengths longer than 350, 470, and 540 nm were adjusted to 1.5 mW cm^{-2} using stainless mesh filters. Under photoirradiation at wavelengths longer than 350 nm, water contact angles on both S-doped and pure TiO_2 thin films decreased rapidly and became lower than 5°. The rate of changes in water contact angle of an S-doped TiO_2 thin film is slightly slower than that of a pure TiO_2 thin film. The final water contact angle on an S-doped TiO_2 thin film is the same as that on a pure TiO_2 thin film. Under visible light irradiation at wavelengths longer than 470 nm, water contact angles on the pure TiO_2 thin film did not change. On the other hand, the critical water contact angles of an S-doped TiO_2 thin film decreased to 15° under visible light irradiation at wavelengths longer than 470 nm for 1 h. In addition, a decrease in the water contact angle of an S-doped TiO_2 thin film was observed visible light irradiation at wavelengths longer than 540 nm for 3 h. Water contact angle of an S-doped TiO_2 thin film reached to 15°.

Under UV light irradiation, surface properties of pure TiO_2 and S-doped TiO_2 thin films became super hydrophilic nature (water contact angle $<5°$ as shown in Fig. 5(a)). These results suggested that surface roughness and densities of the thin films were thought to be independent of photoinduced hydrophilic properties of the surface of TiO_2 thin films. Because water contact angles of pure TiO_2 and S-doped TiO_2 thin films reached to 1°, structural changes in the surface crystal lattice caused the photoinduced hydrophilic conversion of TiO_2 under UV irradiation.

On the other hand, under visible light irradiation, water contact angle reached to 15° as shown in Figs. 5(b) and (c). The value is bigger than that in the case of TiO_2 thin film under UV irradiation. These results suggested that organic contaminants on the surface of TiO_2 thin films were thought to be only removed under visible irradiation.

3.3 Photocatalytic activity of S-doped TiO_2 thin films for decomposition of ALD

Since a photocatalytic reaction takes place on an irradiated TiO_2 surface, adsorption of the reactant on the TiO_2 surface is generally considered to be necessary for accomplishing the reaction. Therefore, it is important to know the adsorption behavior of the reactant on the TiO_2 surface. Before photoirradiation, the reaction vessel containing TiO_2 thin films and ALD was kept in a dark condition at room temperature until the absorption equilibrium of ALD in gas phase was reached.

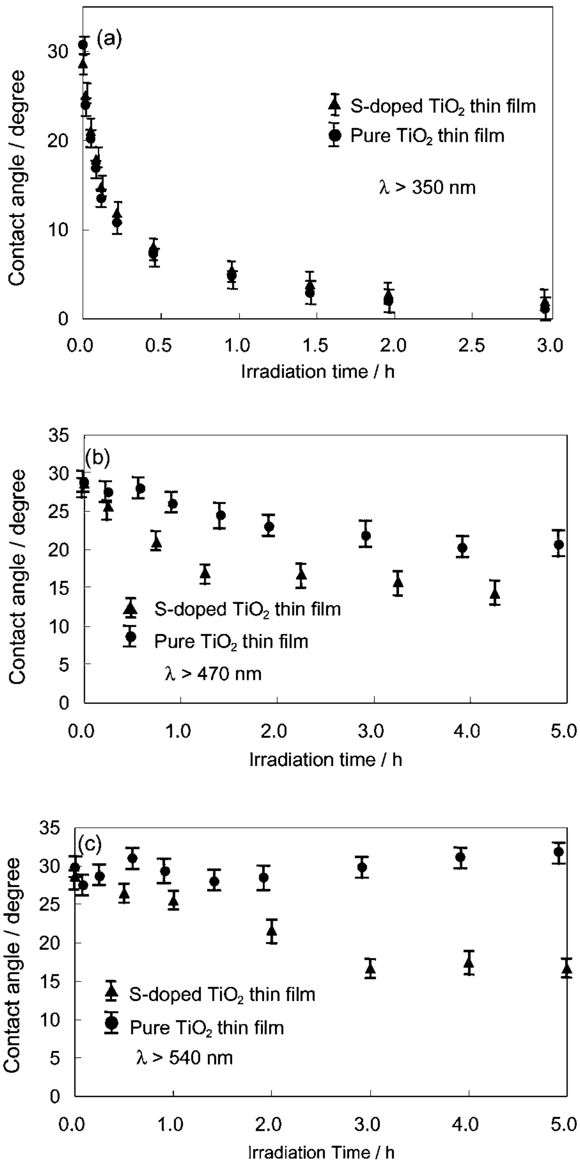

Fig. 5. Changes in water contact angles of S-doped TiO_2 and pure TiO_2 thin films under photoirradiation with a wide range of wavelengths. (a) Under photoirradiation at wavelengths longer than 350 nm, (b) Under photoirradiation at wavelengths longer than 470 nm, (c) Under photoirradiation at wavelengths longer than 540 nm.

Figure 6 presents a typical experimental data set showing the change in concentrations of ALD and CO_2 in the reactor as a function of illumination time. The decrease in ALD concentration and increase in CO_2 concentration with photoirradiation time showed that TiO_2 thin films had activities for degradation of ALD. After prolonged photoirradiation, ALD was completely converted to CO_2. During the photoirradiation, no other decomposition products (or intermediates) were detected in the gas phase within the experimental sensitivity in the present work. However, the possibility of generation of rather stable intermediates such as acetic acid is indicated by the discrepancy between rate constants for degradation of ALD and CO_2 evolution.

The rate constant for degradation of ALD using an S-doped TiO_2 thin film is smaller than that using a pure TiO_2 thin film under photoirradiation at wavelengths longer than 420 nm as shown in Fig. 6. The activity of a pure TiO_2 thin film for CO_2 evolution as a result of degradation of ALD is also higher than that of an S-doped TiO_2 thin film. However, no activity of a pure TiO_2 thin film for degradation of ALD was observed under visible light irradiation at wavelengths longer than 420 nm. The S-doped TiO_2 thin film showed a fairly high photocatalytic activity for degradation of ALD at wavelengths longer than 420 nm. Furthermore, the S-doped TiO_2 thin film retained a rather high photocatalytic activity for evolution of CO_2 generated from decomposition of ALD under visible light irradiation.

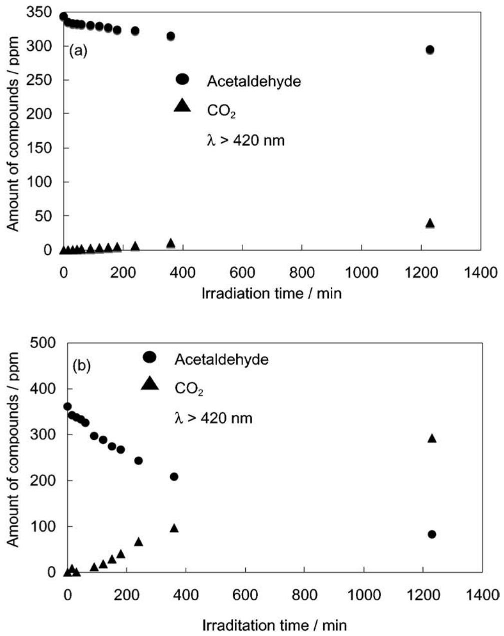

Fig. 6. Changes in concentration gas-phase ALD and CO_2 as a function of irradiation time during the decomposition of ALD under photoirradiation at wavelengths longer than 420 nm. Light intensity, 2.0 mW/cm^2; (●) ALD, (▲) CO_2. (a) Pure TiO_2 thin film, (b) S-doped TiO_2 thin film.

During decomposition of ALD, oxidized intermediates such as acetic acid obtained from oxidation of ALD, which are more stable than ALD, were thought to have accumulated on the surfaces of TiO_2 nanoparticles. This condition retards decomposition of ALD because stable reaction intermediates occupy the active sites on the surfaces of TiO_2 nanoparticles. The discrepancy between the time profiles of degradation of ALD and CO_2 evolution is due to the generation of stable reaction intermediates that are hardly oxidized compounds compared to ALD.[25)]

4. Conclusion

Uniformly dispersed S-doped TiO_2 and pure TiO_2 aqueous coating solutions were prepared by mixing powdered S-doped TiO_2 or pure TiO_2 powders having an anatase phase with a dispersing reagent (POIZ). Thin films of S-doped TiO_2 and pure TiO_2 were obtained from the aqueous coating solutions by using a spin coater. Under visible light irradiation, decrease in water contact angle on S-doped TiO_2 was observed. However, the pure TiO_2 thin film did no show photoinduced hydrophilicity under the same condition.

Photocatalytic degradation of ALD on an S-doped TiO_2 thin film showed activity similar to that on a pure TiO_2 thin film under photoirradiation at wavelengths longer than 350 nm. Under visible light irradiation, only the S-doped TiO_2 thin film showed photocatalytic activity for degradation of ALD in gas phase.

Acknowledgements This work was supported by a Grant-in-Aid for Scientific Research from the Ministry of Education, Culture, Sports, Science and Technology (MEXT) of the Japanese Government and Nissan Science Foundation.

References

1) Fujishima, A., Hashimoto, K. and Watanabe, T., "TiO_2 Photocatalysis Fundamentals and Applications," BKC Inc. (1999).

2) Wang, R., Hashimoto, K., Fujishima, A., Chikuni, M., Kojima, E., Kitamura, A., Shimohigoshi, M. and Watanabe, T., *Nature*, Vol. 388, pp. 431–432 (1997).

3) Wang, R., Hashimoto, K., Fujishima, A., Chikuni, M., Kojima, E., Kitamura, A., Shimohigoshi, M. and Watanabe, T., *Adv. Mater.*, Vol. 10, pp. 135–138 (1998).

4) Sitkiewitz, S. and Heller, A., *New J. Chem.*, Vol. 20, pp. 233–241 (1996).

5) Sopyan, I., Watanabe, M., Murasawa, S., Hashimoto, K. and Fujishima, A., *J. Photochem. Photobiol. A*, Vol. 98, pp. 79–86 (1996).

6) Sawunyama, P., Jiang, L., Fujishima, A. and Hashimoto, K., *J. Phys. Chem. B*, Vol. 101, pp. 11000–11003 (1997).

7) Romeas, V., Pichat, P., Guillard, C., Chopin, T. and Lehaut, C., *New J. Chem.*, Vol. 23, pp. 365–373 (1999).

8) Romeas, V., Pichat, P., Guillard, C., Chopin, T. and Lehaut, C., *Ind. Eng. Chem. Res.*, Vol. 38, pp. 3878–3885 (1999).

9) Minabe, T., Tryk, D. A., Sawunyama, P., Kikuchi, Y., Hashimoto, K. and Fujishima, A., *J. Photochem. Photobiol. A*, Vol. 137, pp. 53–62 (2000).

10) Kikuchi, Y., Sunada, K., Iyoda, T., Hashimoto, K. and Fujishima, A., *J. Photochem. Photobiol. A*, Vol. 106, pp. 51–56 (1997).

11) Sakai, N., Wang, R., Fujishima, A., Watanabe, T. and Hashimoto, K., *Langmuir*, Vol. 14, pp. 5918–5920 (1998).

12) Wang, R., Sakai, N., Fujishima, A., Watanabe, T. and Hashimoto, K., *J. Phys. Chem. B*, Vol. 103, pp. 2188–2194 (1999).

13) Watanabe, T., Nakajima, A., Wang, R., Minabe, M., Koizumi, S., Fujishima, A. and Hashimoto, K., *Thin Solid Films*, Vol. 351, pp. 260–263 (1999).

14) Miyauchi, M., Nakajima, A., Fujishima, A., Hashimoto, K. and Watanabe, T., *Chem. Mater.*, Vol. 12, pp. 3–5 (2000).

15) Hata, S., Kai, Y., Yamanaka, I., Oosaki, H., Hirota, K. and Yamagishi, S., *JSAE Rev.*, Vol. 21, pp. 97–102 (2000).

16) Serpone, N. and Pelizzetti, E., "Photocatalysis Fundamentals and Applications," Wiley (1989).

17) Ollis, D. F. and Al-Ekabi, H., "Photocatalytic Purification and Treatment of Water and Air," Elsevier (1993).

18) Sakatani, Y. and Koike, H., Japan Patent, P2001-72419A (2001).

19) Asahi, R., Ohwaki, T., Aoki, K. and Taga, Y., *Science*, Vol. 293, pp. 269–271 (2001).

20) Irie, H., Washizuka, S., Yoshino, N. and Hashimoto, K., *Chem. Commun.*, Vol. 11, pp. 1298–1299 (2003).

21) Ohno, T., Mitsui, T. and Matsumura, M., *Chem. Lett.*, Vol. 32, pp. 364–365 (2003).

22) Ohno, T., Akiyoshi, M., Umebayashi, T., Asai, K., Mitsui, T. and Matsumura, M., *Appl. Catal. A, Gen.*, Vol. 265, pp. 115–121 (2004).

23) Ohno, T., Tsubota, T., Nishijima, K. and Miyamoto, Z., *Chem. Lett.*, Vol. 33, pp. 750–751 (2004).

24) Ohno, T., Tsubota, T., Toyofuku, M. and Inaba, R., *Catal. Lett.*, Vol. 98, pp. 255–258 (2004).

25) Muggli, D. S., McCue, J. T. and Falconer, J. L., *J. Catal.*, Vol. 173, pp. 470–483 (1998).